ISSN 2007-9737

Detection and Classification of Multiple Sclerosis from Brain MRIs by Using MobileNet 2D-CNN Architecture

Sudhanshu Saurabh[1, 2,*], P. K. Gupta[3]

[1] Jaypee University of Information Technology, Wakanaghat, India

[2] East Point College of Engineering and Technology, Bangalore, India

[3] Mohan Babu University, School of Computing, Department of Data Science, India

ssmiete@gmail.com, pkgupta@ieee.org

Abstract. Deep learning-based object detection and classification have been widely investigated for neuroimaging. Magnetic resonance imaging (MRI) data serve as a diagnostic tool for the detection and classification of brain disorders such as Parkinson's, Alzheimer's disease (AD), and Multiple Sclerosis (MS). In addition, the use of the Convolutional Neural Network (CNN) framework helps in the development of predictive models from the available MRI images. This work aims to develop a CNN-based model with a pre-trained MobileNet model to detect and classify multiple sclerosis using the MRI image dataset. In this article, we have proposed a pre-trained MobileNet-2D-CNN architecture for the accurate prediction of multiple sclerosis from various MRI images. Initially, the proposed model extracted images from MRI images of the affected patient with MS and healthy control. We used MRI images to train the MobileNet-2D-CNN model to identify the MS features map that predicts MS. The proposed architecture has been validated on standard MRI scans. We also performed a class activation map for the interpretation of the prediction provided by the proposed model, which represents the behavior of neurons in the early stages. The proposed approach achieves a classification precision of 98.15% and AUC=1.00.

Keywords. CNN, deep learning, feature map, mobilenet, MRI, multiple sclerosis.

1 Introduction

Automatic detection and classification of various brain disorders such as Alzheimer's disease (AD), brain tumors, multiple sclerosis, schizophrenia, and Parkinson's have become a major concern in modern healthcare. Multiple sclerosis (MS) is an irreversible degenerative brain disorder characterized by loss of cognitive function and has no proven cure. MS is a condition and demyelinating disease of the central nervous system that affects mainly the brain and spinal cord and damages the protective covering of nerve fibers resulting in vision loss, depression, decreased sensitivity, mobility problems, and several other issues related to thinking, learning, and planning [3, 32]. The progression of MS can be classified into two subsequent classes known as Benign and Malignant. These two terms represent the severity of MS, where benign MS represents a mild course of multiple sclerosis and malignant MS represents a significant level of disability in various patients. To examine the extent of psychometric properties, the Expanded Disability Status Scale (EDSS) is used as an indicator for patients affected

ISSN 2007-9737

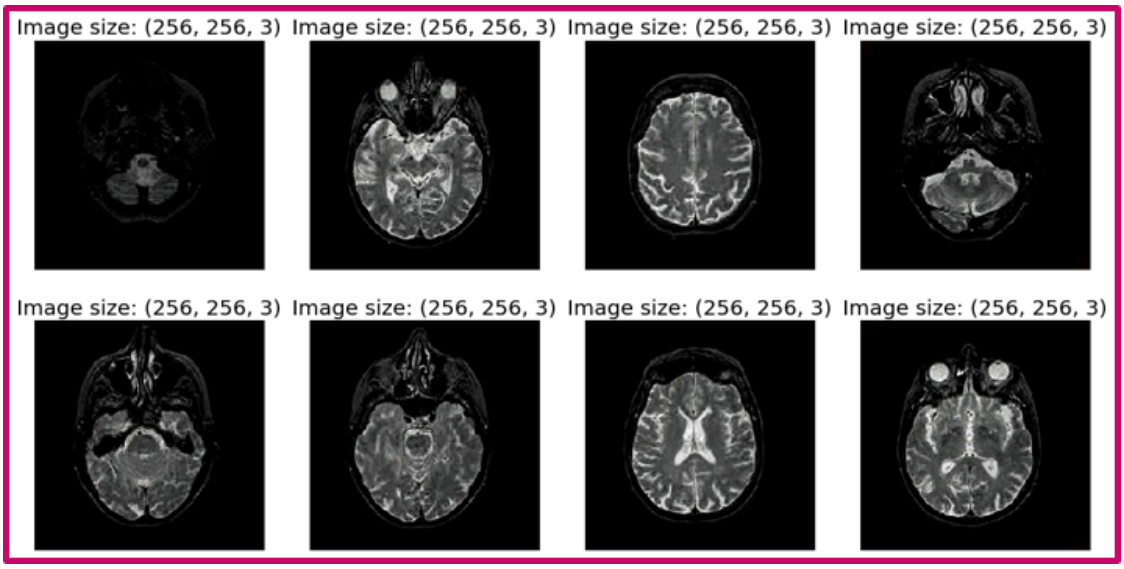

(a)

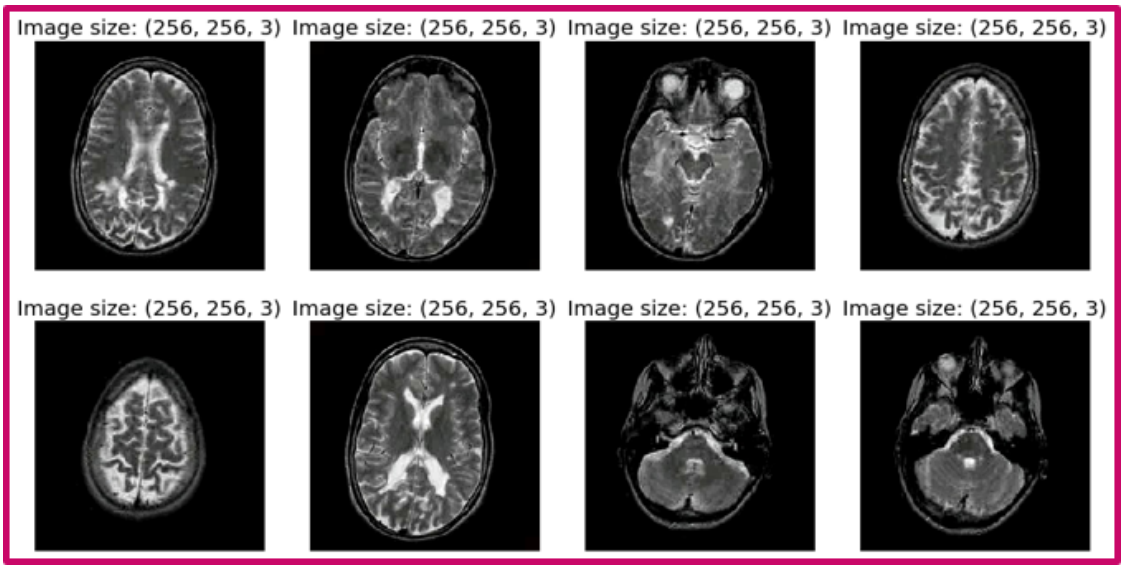

(b)

Fig. 1. Sample image of brain MRI scan dataset (a) Normal healthy control (b) Multiple sclerosis (MS)

by MS [30]. Saliency maps are applied to healthy and Alzheimer's fMRI images by the authors in [25].

Among the various medical imaging techniques, magnetic resonance imaging is one of the most efficient and suitable neuroimaging methods for detecting the presence of white matter lesions in the brain that suggest MS and also effectively diagnose the abnormality in the brain region due to MS [4, 18]. The appearance and shape of the lesions can vary during the MRI scan at each time point [4, 5]. Moreover, measuring the growth of the lesion by using the white signals visible in various MRI scans is another challenging task, as in some MRI scans the lesion disappears at a single time

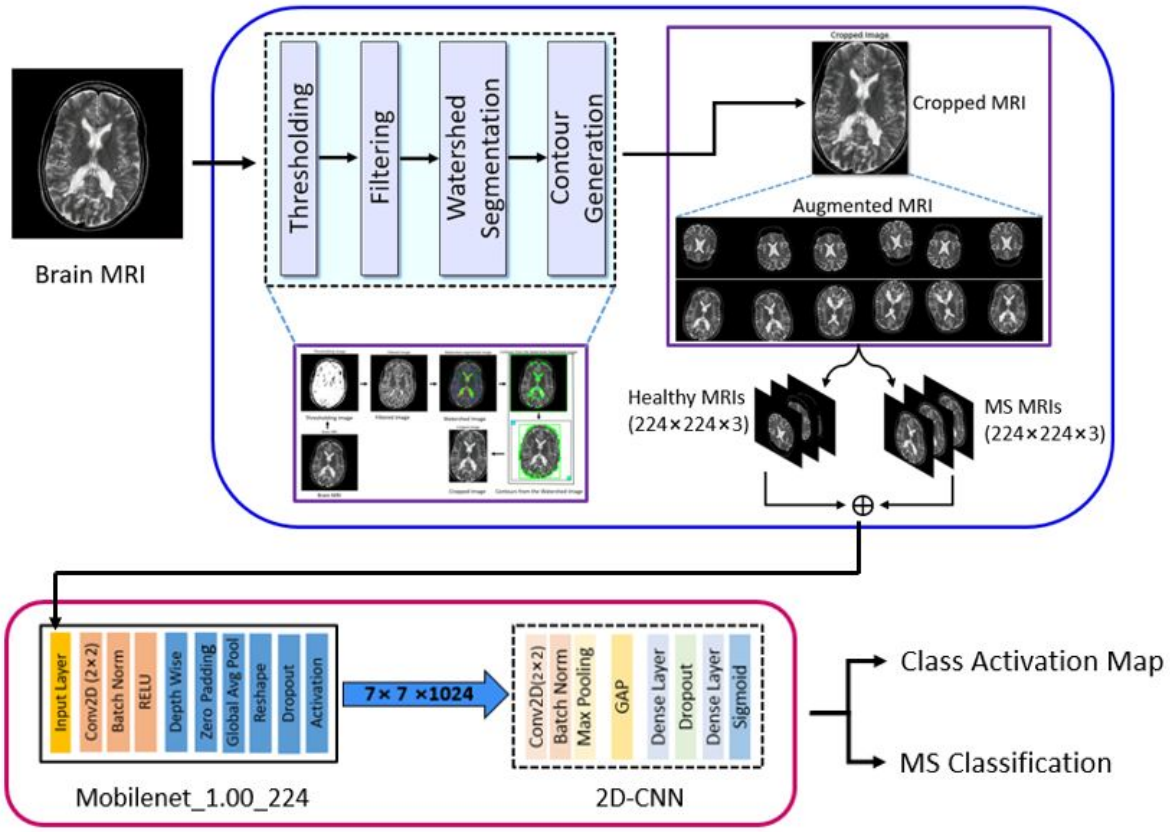

Fig. 2. Proposed architecture using brain MRI images for multiple sclerosis detection and classification

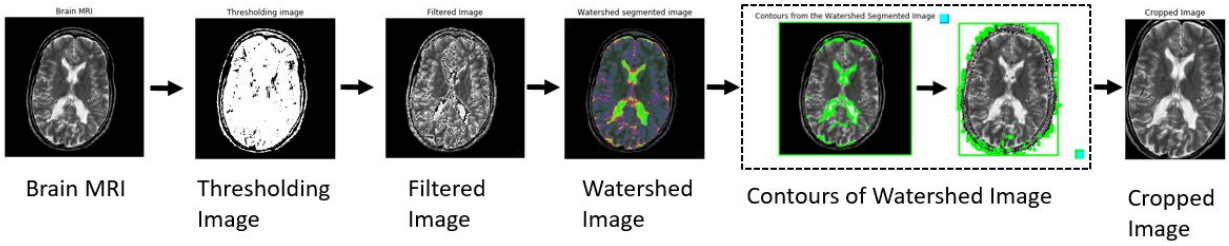

Fig. 3. Preprocessing steps involve cropping the brain MRI image

point or lesion time point (LTP) [12]. As shown in Fig. 1, magnetic resonance imaging is used to detect the presence of a white matter lesion in the specific region of the brain to find the MS lesion.

Through experimental studies, deep learning networks such as LiviaNet, HyperDenseNet, and the Convolutional Neural Network (CNN) are widely used for the detection and classification of various neural syndromes [1, 8]. In this work, an experiment is presented to perform a two-dimensional CNN (2D-CNN) model that selects the slices and training input. In the first case, we perform numerical and gradient-based learning at each stage of the densely connected network and are treated as a feature extraction engine that processes a set of effective features

(a)

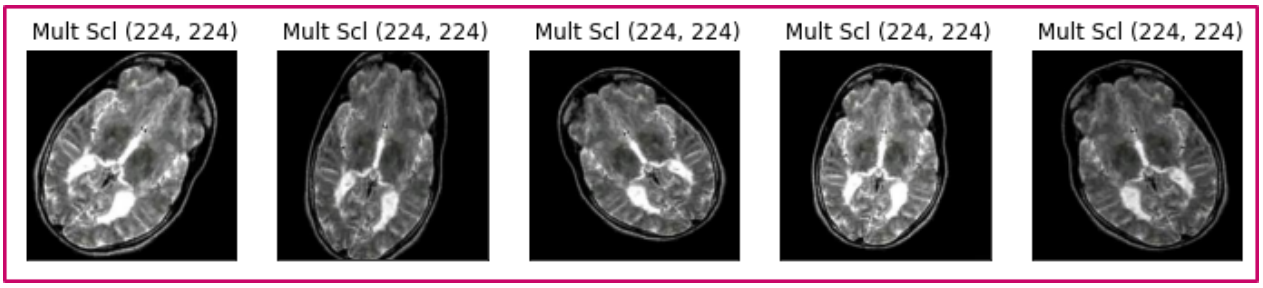

(b)

Fig. 4. Augmented image of brain MRI scan dataset (a) Augmented healthy brain MRI (b) Augmented multiple sclerosis brain MRI

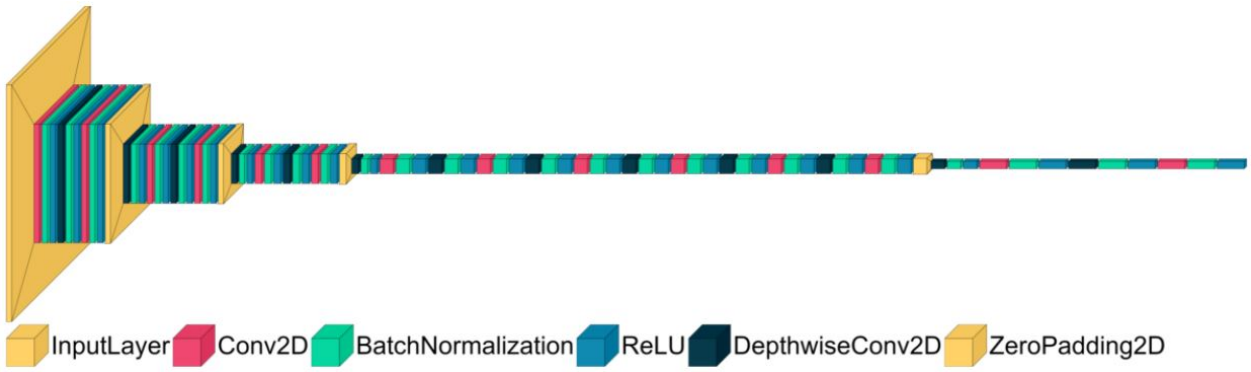

Fig. 5. MobileNet architecture

of the MRI dataset. In this study, we have demonstrated the feature extraction of MRI images from the proposed MobileNet-2D-CNN architecture. The size of the MobileNet network is small, which reduces the computation time and reduces the problem of overfitting [17, 29].

Once the feature extraction process is completed, then fed to the 2D-CNN which constructs the feature map from the input segment through the convolutional layer, the max pooling layer, and the fully connected layer handles various 3D-MRI images for detection and classification of MS. The main highlights of this research study are as follows:

– Detect and classify the MS lesion from the MRI images by using the deep learning method.

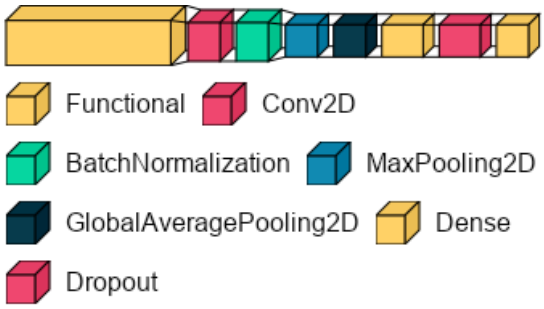

Fig. 6. Proposed MobileNet-2D-CNN model

– The proposed model trains the network using the MRI images that show the high signal in the periarterial white matter on the T2 weighted image data.
– Generates the class activation map, which provides the visual diagnosis and classification of MS lesions.

2 Related Work

Various studies have been conducted with essential findings that discriminate MS disease from healthy control [18]. These studies focus on the use of machine learning and deep learning-based frameworks and consider MRI scans to find the severity of the disease.

The authors of [4] have considered a CNN architecture based on deep learning and used a vast volume of brain MRI data voxel data for further analysis of MS lesion segmentation. Using 4D-fMRI images, the authors of [26] developed a deep learning model and a reshaping algorithm for the classification of ADHD conditions.

The authors in [20]have proposed a CNN-based MS classifier known as DeepScan for the identification of MS lesions. In [1], the authors have discussed the various deep learning-based techniques that consider the publicly available Brain MRI image segmentation dataset.

In [2], authors have discussed the framework known as an ITK toolkit and applied the watershed transform method for the detection of region boundaries in MRI scans. In [27], the authors have focused on effective neural network training to classify MRI images with limited data and to prevent overfitting the network.

They have simply adopted the proposed model to increase the size of the dataset by using image data augmentation that improves accuracy. In [17], the authors have used precision reduction methods to reduce spatial resolution in different features of the feature map generated by the LeNet-5 network.

The authors in [22, 23], discussed the discrimination of the region in the input image, and the class activation map is influenced by the deep learning model for classification. The authors of [10, 11] have discussed various predictive frameworks and algorithms for the classification and detection of various diseases.

3 Materials and Methods

3.1 Data Analysis

The experimental MRI dataset used in this study consists of unlabeled brain images from MRI scans to detect and classify MS injury from the healthy control.

This data set is acquired from the publicly available Whole Brain Atlas[1]. This data set consists of standard slices and axial orientations of various MRI scans of the brain. Furthermore, the abnormalities appearing in the data set are based on pre-arterial white matter, pre-gadolinium, and post-gadolinium in the T1 and T2-weighted MRI images, respectively.

[1] www.med.harvard.edu/AANLIB/

Table 1. Proposed architecture of MobileNet-2D-CNN

OPERATION	DATA DIM	WEIGHTS(N)
Input Layer	$224 \times 224 \times 3$	–
MobileNet_1.00_224	$7 \times 7 \times 1024$	3228864
Conv2D	$5 \times 5 \times 32$	294944
Batch Normalization	$5 \times 5 \times 32$	128
Max Pooling 2D	$1 \times 1 \times 32$	–
Global Avg Pooling 2D	32	–
Dense	–	8448
ReLU	256	–
Dropout	256	–
Dense	–	257
Sigmoid	1	–

This data set also consists of distinct 4D images of brain magnetic resonance imaging scans of 30-year-old patients acquired with axial T1-weighted data. These brain magnetic resonance images show a high signal in white matter in the T2-weighted images.

Here, the MRI images obtained from the normal control and MS subjects are four-dimensional (4D) brain images. These 4D images are defined as ($256 \times 256 \times 22 \times 3$) along with the dimension of the pixel ($1 \times 1 \times 1$) mm^3 and the size of the voxel 3 mm^3. The 4D MRI image data with 22 slices and a voxel size of 3 mm^3 are isotropic for the detection and classification of MS from the normal control. The ratio of MRI images of patients affected with MS with healthy subjects is 22:52.

3.2 Methodology

In this section, we have described the proposed model for the detection and classification of MS lesions, as shown in Fig. 2.

The proposed model consists of three modules, i.e. Image preprocessing, MobileNet, and 2D-CNN. The detailed functioning of these modules is discussed in the following subsections. The architecture of the pre-trained MobileNet convolutional neural network is used for the initial stage of dataset training, the MobileNet contains a stack of layer blocks named as convolutional layer, Batch Normalization, Depthwise convolutional layer followed by Global Average Pooling (GAP) layer. Using the MobileNet to classify the natural images is not similar to the numerical data array, so more convolutional blocks are required to properly tune the brain MRI image dataset.

3.2.1 MRI Pre-processing

Here, we apply various preprocessing steps, such as adjusting, readjusting, and enhancing, to the MRI images before feeding them into the MobileNet-2D-CNN model. These preprocessing steps are discussed as follows:

3.2.2 Cropping and Resizing

Due to the computational task and limitation of fitting a complete MRI image into the model, we reduce the size of the brain image from ($256 \times 256 \times 3$) to ($131 \times 176 \times 3$). The target size of the brain image is selected in such a way that includes the most of the brain image scanned by the scanner after performing the cropping and resizing effect on the original brain image. In this work, we have worked with the data-driven strategy and performed the cropping on the Brain MRI scans to remove the undesired regions.

– Edge detection: To compute the gradient magnitude of the Brain image, we have applied the Sobel edge detection method to obtain minimum and maximum gradient, inside and at the edge of the various MRI scans of the brain as shown in Fig. 3.

– Thresholding: Once the edge is detected, we perform the thresholding that divides the pixel of the grayscale image and converts the MRI scans into binary images [21].

– Filtering: Further, filtering uses the Sobel filter and removes the noise of low frequencies from the MRI images.

– Segmentation and Contour: Here, we apply a watershed algorithm on the filtered image that extracts the segmented regions by the finding of watershed lines [2].

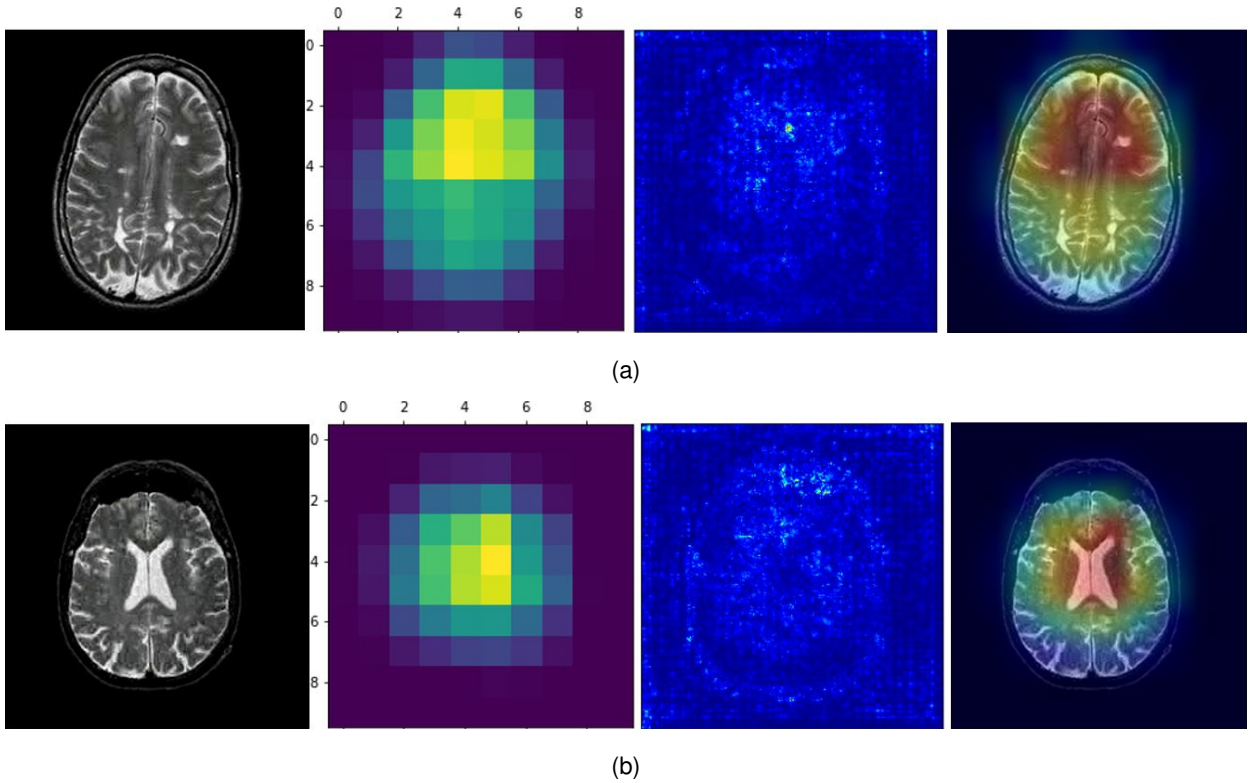

(a)

(b)

Fig. 7. Visualization of multiple sclerosis affected vs. healthy MRI image size (224×224) on the proposed model (a) Class activation map of multiple sclerosis (b) Class activation map for healthy brain MRI

Choosing the Largest Contour of the watershed transformed image and applying grayscale to convert it into binary images [31]. The main steps of the MRI image cropping and resizing procedure are described below.

– Step-1: We have considered the MRI dataset of MS-affected and healthy subjects. Here, the dimension of each input image is (256×256×3).

– Step-2: Further, we have applied the Binary Thresholding on the input image.

– Step-3: Applies the Sobel filter for filtering the thresholding image where the gradient operator are:

$$G_x = \text{[-1, 0, 1]}, \quad \text{[-2, 0, 2]}, \quad \text{[-1, 0, 1]}$$

$$G_y = \text{[1, 2, 1]}, \quad \text{[0, 0, 0]}, \quad \text{[-1, -2, -1]}$$

– Step-4: Applies the watershed transformation for segmenting the region in the filtered MRI image. This provides an accurate and effective segmentation of input MRI images.

– Step-5: Applies the chain approximation algorithm on the segmented MRI image and generates green points on all the contours.

– Step-6: Detect each contour find the largest contour on the MRI image and apply crop operation on the largest contour to obtain cropped MRI image of dimension (131×176×3).

3.2.3 Image Augmentation

Applying the MobileNet-2D-CNN model to an MRI image of the brain is one of the challenging tasks as a limited amount of training dataset is available. To overcome this problem, data augmentation

Table 2. Generated feature map from activation channels

Activation Layer	No. of Feature Map
Mobilenet_1.00_224	32
Conv2d	128
Batch_Normalization_1	256
Max_Pooling2d_1	512
GlobalAveragePooling2D	512

techniques are used that enhance the size and quality of the training dataset and also improve the performance of the proposed model.

The image augmentation strategy that the network will use for more training data also reduces the overfitting of the proposed model. Image augmentation comes from transformation, color space, random cropping, orientation, mixing images, kernel filters, etc.

The classification accuracy of the deep learning model performs much better in the augmented test data set [27]. We have performed data augmentation on magnetic resonance images, using ImageDataGenerator API from Keras inside the Tensorflow 2.5 before we feed into the MobileNet network.

The augmentation of images includes factors such as rotation, shifting, shear, horizontal flip, vertical flip, and brightness that generate the new training dataset as shown in Fig. 4.

The augmentation operation is performed by random rotation by 45^0 and then applies to the shift, shearing with the rotated images, and then applying horizontal and vertical flipping of the transformed image. Finally, resize the MRI images that correspond to the input size of the MobileNet model, that is, (224×224) pixels.

3.2.4 MobileNet Network Architecture

The Standard convolution model uses a layer stack in which the CNN image features include channel-wise and spatial-wise information. Unlike spatial convolution, depth convolution deals with spatial dimension and depth dimension or the number of channels [14].

A deep separable convolution commonly known as a separable convolution is related to the grouped convolution and inception modules of the Inception family [7]. The depth-wise convolution is followed by a point-wise convolution with (1 $\times$ 1) window and project the new channel space. In MobileNet, the separable convolution allows one to build an image classification model such as MobileNet_224.

In this work, we have used MobileNet as it is a lightweight CNN architecture built primarily from deep separable convolution, as shown in Fig. 5. The small network and low latency achieve good efficiency relative to standard convolution.

The shape of the image has three dimensions of the input feature map F to the convolution layer is (spatial map $\times$ height $\times$ input depth) produces another feature map G that is defined as (spatial map $\times$ height$\times$ output depth) and the size of the convolution kernel K is given as ($D_K \times D_K \times M \times N$) where ($D_K \times D_K$) corresponds to squared spatial dimension of kernel and M, and N are input and output depths respectively.

The depth-wise convolutional kernel performs a single convolution on each channel and can be defined as follows:

$$X_{k,\,l,\,m} = \sum_{i,j} K_{i,\,j,\,m} \cdot F_{k+i-1,\,i+j-1,\,m}. \qquad (1)$$

The computational cost of the depth-wise convolution is calculated as:

$$D_K \cdot D_K \cdot M \cdot N \cdot D_F \cdot D_F, \qquad (2)$$

where D_K, D_F, M and N are dimensions of the convolutional kernel, spatial width, height, input channel, and output channel, respectively.

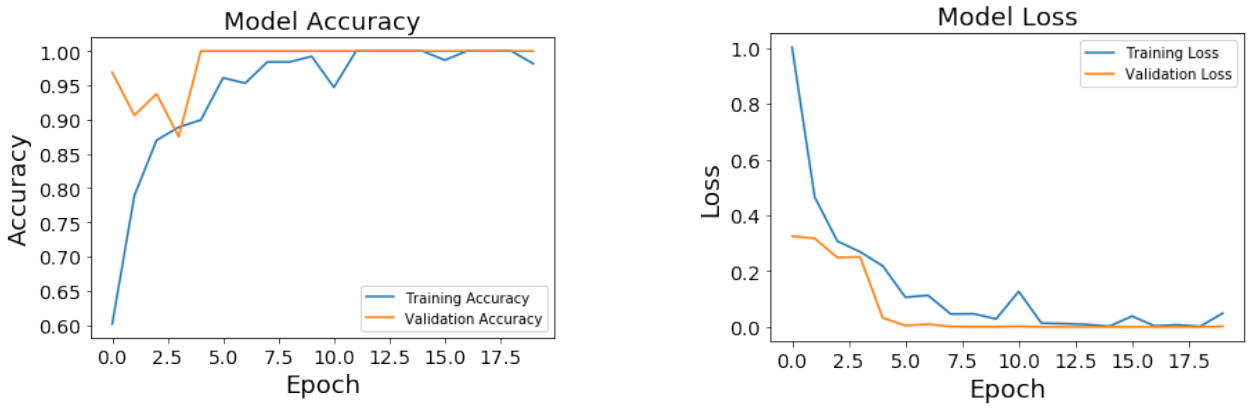

Fig. 8. Learning curve of the proposed model (a)Training and validation accuracy (b) Training and validation loss

3.2.5 Proposed MobileNet-2D-CNN Architecture

The architecture of the proposed MobileNet 2D CNN is shown in Fig. 5 which is based on a separable filter for depth and performs a single convolution for each input channel. For the target network adding one convolution layer followed by one maximum grouping layer and two fully connected layers of size 256 and 2, the dropout is 0.5% and we have used the root mean square propagation RMSprop optimizer [9] to train the model with the learning rate being 0.0001. Here, RMSprop optimizer is defined as per following:

$$E[g^2]_t = 0.9E[g^2]_{t-1} + 0.1g_t^2, \tag{3}$$

$$\theta_{t+1} = \theta_t + \frac{\eta}{\sqrt{E[g^2]_t + \epsilon}} g_t, \tag{4}$$

where $E[g^2]_t$ is the running average in time t depending on momentum γ=0.9 [24] and the default value of the learning rate η = 0.001 on the previous average $E[g^2]_{t-1}$, gradient of the objective function is denoted by g_t for the update parameter θ at every time step t.

The combination of these 2D-CNN layers is applied along the MobileNet network. The features generated from the MobileNet are further fed to a shallow custom CNN architecture, as shown in Fig. 2. The obtained output shape of the MobileNet MRI image will be input to 2D-CNN.

The proposed MobileNet-2D-CNN model is trained in 20 epochs since we used a training and testing scheme of 80-20%. The proposed model shows an accuracy of 98.15%. Since the data set used in this research is gray images, therefore, the value of pixels in the MRI images is between 0 and 255. The visualization of MRI images shows how perfectly the proposed model extracts the features for the MS classification.

3.3 Class Activation Map (CAM)

For a specific class, the class activation map with the global average grouping is applied to the proposed MobileNet-2D-CNN model. These weighted activation maps are generated by the hidden layers of the MRI images.

The network visualization pattern is activated by each unit of the network [16]. CNN learns while being trained to recognize the object [15]. The features obtained are fed into the fully connected layer (FC), regulated by the Softmax activation function, and provide the result of the calculated probabilities for further classification [28].

We have illustrated the activation from the convolutional layer. Consider the activation k of the convolution layer at the location $(i,\ j)$, then the activation function for the MRI image will be denoted as $f_k(i,\ j)$.

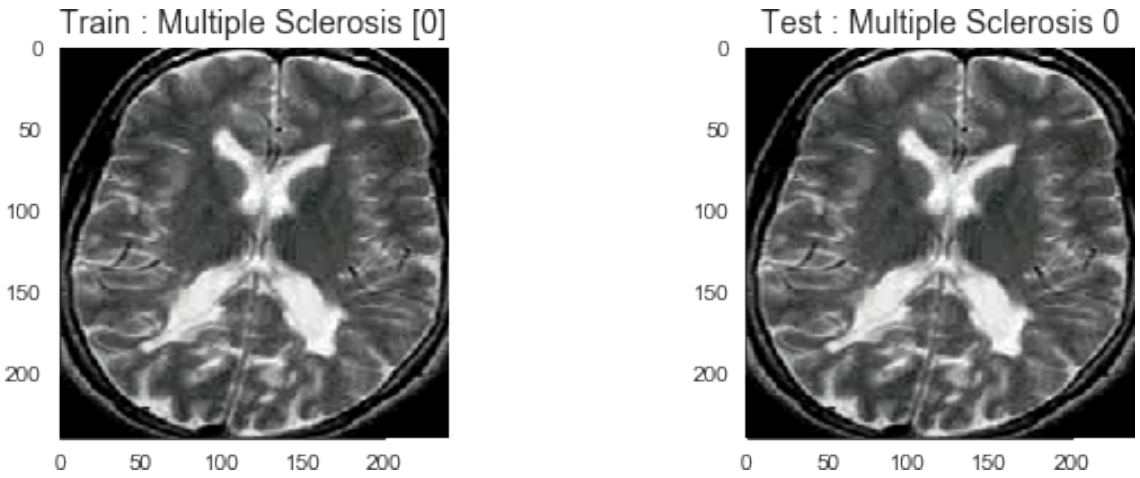

Fig. 9. Classified MS affected brain MRI

Here, global average pooling (GAP) at activation k is represented by G_k as shown in Eq. 5:

$$G_k = \sum_{i,j} f_k(i,j). \tag{5}$$

The softmax activation function is used for the computation of class label C_i probablities P_{C_i} [16]:

$$\sigma_{C_i} = \sum_k \omega_k^{C_i} G_k, \tag{6}$$

where, the weight vector $\omega_k^{C_i}$ of the network corresponds to the class label C_i at the activation k. Therefore class probablities P_{C_i} and the softmax activation function σ_{C_i} is defined as:

$$P_{C_i} = \frac{\exp(\sigma_{C_i})}{\sum_{C_i} \exp(\sigma_{C_i})}, \tag{7}$$

$$\sigma_{C_i} = \sum_k \omega_k^{C_i} \sum_k f_k(i,j). \tag{8}$$

The class activation map (CAM) is obtained by using the weighted feature map governed by the softmax weight σ_{C_i} that classifies the heat map corresponding to a specific class.

3.3.1 Visualization of Class Activation

In the forward network, the MRI image input $f_k(i,j)$ with height h, width w, and depth d is processed through the proposed MobileNet–2D-CNN model. The MRI image tensor $(h \times w)$ maps each pixel dimension to its corresponding color class C_i. Additionally, the classifier maps the input MRI image to the class saliency map $H \in \mathbb{R}^{h \times w}$ and applies the activation function G_k to each pixel of the input image $f_k(i,j)$. The weighted neurons are computed as the gradient of the softmax activation function σ_{C_i} with respect to the activation of the feature map f_k from the convolutional layer, as defined below:

$$\omega_k^{C_i} = \left.\frac{\partial \sigma_{C_i}}{\partial f_k}\right|_{f_k(i,j)}. \tag{9}$$

Taking the partial derivative of G_k with respect to $f_k(i,j)$, that is:

$$\frac{1}{N} = \frac{\partial G_k}{\partial f_k(i,j)}, \tag{10}$$

$$H = \text{relu}\left\{\sum_k \omega_k^{C_i} f_k(i,j)\right\}. \tag{11}$$

This formulation of the computation allows us to generate the visualization of the saliency map of the multiple sclerosis (MS) MRI image.

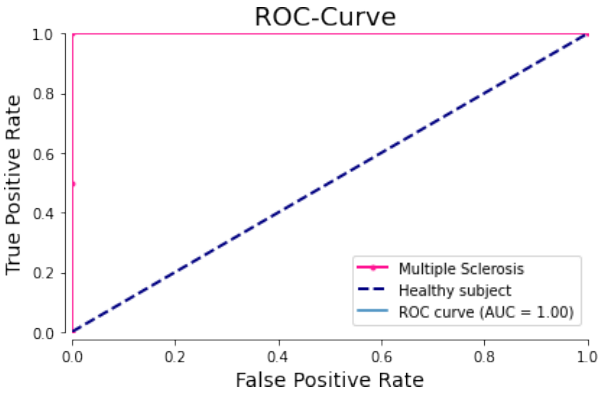

Fig. 10. ROC curve estimates the AUC between 0 - 1 with the binary classifier and plots the true positive rate vs. false positive rate

4 Experiments and Results

The proposed model evaluates the classification of Multiple Sclerosis present in MRI images. Based on the formulae described above, the proposed model considers the size of the MRI images (224×224 ×3) that includes 475 training images for the training set, 19 images for validation to perform the support dataset and 95 images for the test dataset. We have observed the hidden layer gradient images, the MS classification, and the performance of the proposed model. We begin by presenting the class activation map using gradients to interpret the proposed network, experimental training strategy, and classification followed by model evaluation.

4.1 Implementation Details

The experimental setup of the MobileNet-2D-CNN model has been designed and trained on MRI images as shown in Fig. 2. The MobileNet input layer has a size of (224×224×3) to preprocess the MRI image data. The next layer is the 2D convolutional layer with kernel size (3×3) it is determined the receptive field that received input with the dimension of (7×7×1024) then applying the ReLU activation function to the output of the convolution, after that the batch normalization layer takes the input size of the data (5×5×32) it is used to normalize the data and reduces the data loss between the processing layers, a max pooling layer is used to downsample to the output of size (1×1×32). The global average pooling layer converts the 3D feature map matrix from the maximum pooling layer to the vector 1D and generates a single feature map.

Subsequently, the two fully connected (FC) layers are used for classification purposes. Here, the first FC layer has 256 output neurons followed by the dropout layer with probability = 0.5, and the next FC layer consists of 256 input neurons with 2 output neurons for the two-class classification.

We have trained the proposed MobileNet–2D-CNN model with the binary cross-entropy loss function and the RMSprop optimizer, where the batch size is 32, and 20 epochs are applied to the MRI image data. To classify MS, the proposed MobileNet 2D-CNN architecture is implemented by using Tensorflow and Keras open source library.

The proposed model is trained on the powerful NVIDIA Geforce GTX 1080 GPU. All parameters used in the proposed network are summarized in Table 1. The classification accuracy obtained from the proposed MobileNet 2D-CNN model is 98.15%. Here, Fig. 8 shows the training and validation accuracy of the proposed model.

4.2 Grad-CAM Visualization

The proposed MobileNet–2DCNN architecture is trained to produce heat maps from input MRI images. These heat maps detect the location of the MS lesion on the MRI image as per Fig. 7. The heat maps generated from the convolutional layer use a single input channel due to grayscale MRI images. Here, the convolutional layer considers the weighted average output.

In each channel, the feature map uses the weight in the FC layer. The softmax layer performs the computation for the class prediction of the heatmaps. The output of a softmax layer gradient with respect to each channel forms a feature map of a specific layer that displays a gradient of the respective output channel. We have obtained feature maps generated from each activated layer as per Table 2.

These gradient feature maps of MRI images are fed into the Global Average Pooling (GAP) layer that considers the size of the MRI image tensor as ($5\times5\times32$) and performs the averaging across the (5×5) convolution. The average value of each of the input channels generates one output channel, i.e. a one-dimensional tensor with 32 images. These weighted feature maps 2D, as generated by the GAP layer, are used as heat maps.

4.3 Classification of MS Lesion

MRI images are classified using the proposed model, which predicts class labels as illustrated in Fig. 9. The model is trained and tested on a dataset of 475 preprocessed MRI images, including both healthy controls and MS-affected individuals. This dataset is split into 80% for training and 20% for testing, with 5% of the training data reserved for validation. The classification utilizes a 2D CNN to identify MS lesions, as demonstrated in Fig. 9.

4.4 Model Evaluation

In the binary classification, the prediction of classes for the computed probabilities is based on the continuous variable. Probability is classified as positive if the computed probabilities $>$ threshold value otherwise negative. The classification performance of the proposed model is measured using the area under the curve (AUC).

The receiver operating characteristic (ROC) curve between the TPR and FPR, computes the area under the ROC curve [6, 19]. The AUC ranges from 0.5 to 1.0, generally interpreted as the probability that the diseased subject is randomly selected which has a higher test value compared to the random selection of the healthy subject [13].

The AUC value measures the overall performance of the classification model. Here, Fig. 9 shows that the classifier of the proposed MobileNet-2D CNN has AUC = 1.00, which shows that the performance of the model is based on the MRI scan data and is perfectly classified by the proposed model. A model with multiple sclerosis is shown by an orange curve that travels from the bottom left to the top right and above the threshold diagonal line.

5 Conclusion and Future Work

We have proposed a MobileNet - 2D-CNN model for the detection and classification of MS-affected lesions in brain MRI images. The proposed model uses the threshold-based extraction method from the MRI image. Further, we have applied the data augmentation methods for generating the dataset during the pre-processing steps.

The learning process of the proposed model depends mainly on the selection of the training data set. Using the augmented data to experiment with our proposed MobileNet–2D-CNN architecture as shown in Fig. 6 generates the gradient class activation map for the detection and classification of MS lesions from MRI images.

The experimental results obtained to find the MS-affected classification from the test dataset are shown in Fig. 8. In these results, we have achieved a classification accuracy of 98.15% from the binary classifier. An ROC curve shows the classification performance with AUC = 1.00.

For both detection and classification, it is expected that an in-depth study can achieve a similar quality of feature that can be achieved by a nonlinear deep learning model. For that reason, future research towards creating a more refined structure that can take the findings forward to the systematic exploration of the lesion map in terms of clinical application.

References

1. **Akkus, Z., Galimzianova, A., Hoogi, A., Rubin, D. L., Erickson, B. J. (2017).** Deep learning for brain MRI segmentation: State of the art and future directions. Journal of Digital Imaging, Vol. 30, No. 4, pp. 449–459. DOI: 10.1007/s10278-017-9983-4.
2. **Beare, R., Chen, J., Adamson, C. L., Silk, T., Thompson, D. K., Yang, J. Y. M., Anderson, V. A., Seal, M. L., Wood, A. G. (2013).** Brain extraction using the watershed transform from markers. Frontiers in Neuroinformatics, Vol. 7. DOI: 10.3389/fninf.2013.00032.

3. **Benedict, R. H. B., Amato, M. P., DeLuca, J., Geurts, J. J. G. (2020).** Cognitive impairment in multiple sclerosis: Clinical management, MRI, and therapeutic avenues. The Lancet Neurology, Vol. 19, No. 10, pp. 860–871. DOI: 10.1016/s1474-4422(20)30277-5.
4. **Birenbaum, A., Greenspan, H. (2017).** Multi-view longitudinal CNN for multiple sclerosis lesion segmentation. Engineering Applications of Artificial Intelligence, Vol. 65, pp. 111–118. DOI: 10.1016/j.engappai.2017.06.006.
5. **Chhatbar, P. Y., Kara, P. (2013).** Improved blood velocity measurements with a hybrid image filtering and iterative Radon transform algorithm. Frontiers in Neuroscience, Vol. 7, pp. 106. DOI: 10.3389/fnins.2013.00106.
6. **Cho, H., Matthews, G., Harel, O. (2018).** Confidence intervals for the area under the receiver operating characteristic curve in the presence of ignorable missing data. International Statistical Review, Vol. 87, No. 1, pp. 152–177. DOI: 10.1111/insr.12277.
7. **Chollet, F. (2017).** Xception: Deep learning with depthwise separable convolutions. IEEE Conference on Computer Vision and Pattern Recognition, pp. 1800–1807. DOI: 10.1109/cvpr.2017.195.
8. **Ding, Y., Acosta-Sánchez, R., Enguix-Chiral, V., Suffren, S., Ortmann, J., Luck, D., Dolz, J., Lodygensky, G. (2020).** Using deep convolutional neural networks for neonatal brain image segmentation. Frontiers in Neuroscience, Vol. 14, pp. 207. DOI: 10.3389/fnins.2020.00207.
9. **Duchi, J., Hazan, E., Singer, Y. (2011).** Adaptive subgradient methods for online learning and stochastic optimization. Journal of Machine Learning Research, Vol. 12, No. 61, pp. 2121–2159.
10. **Gupta, P. K., Ören, T., Singh, M. (2018).** Predictive intelligence using big data and the internet of things. IGI Global.
11. **Gupta, P. K., Tyagi, V., Singh, S. K. (2017).** Predictive computing and information security. Springer Singapore. DOI: 10.1007/978-981-10-5107-4.
12. **Guttmann, C. R., Ahn, S. S., Hsu, L., Kikinis, R., Jolesz, F. A. (1995).** The evolution of multiple sclerosis lesions on serial MR. American Journal of Neuroradiology, Vol. 16, No. 7, pp. 1481–1491.
13. **Hanley, J. A., McNeil, B. J. (1982).** The meaning and use of the area under a receiver operating characteristic (ROC) curve. Radiology, Vol. 143, No. 1, pp. 29–36. DOI: 10.1148/radiology.143.1.7063747.
14. **Howard, A. G., Zhu, M., Chen, B., Kalenichenko, D., Wang, W., Weyand, T., Andreetto, M., Adam, H. (2017).** MobileNets: Efficient convolutional neural networks for mobile vision applications. DOI: 10.48550/arXiv.1704.04861.
15. **Hoyer, L., Munoz, M., Katiyar, P., Khoreva, A., Fischer, V. (2019).** Grid saliency for context explanations of semantic segmentation. Proceedings of the 33rd International Conference on Neural Information Processing Systems, pp. 6462–6473.
16. **Kwaśniewska, A., Rumiński, J., Rad, P. (2017).** Deep features class activation map for thermal face detection and tracking. Proceedings of the 10th International Conference on Human System Interactions, pp. 41–47. DOI: 10.1109/HSI.2017.8004993.
17. **Lecun, Y., Bottou, L., Bengio, Y., Haffner, P. (1998).** Gradient-based learning applied to document recognition. Proceedings of the IEEE, Vol. 86, No. 11, pp. 2278–2324. DOI: 10.1109/5.726791.
18. **Lu, S. Y., Wang, S. H., Zhang, Y. D. (2020).** A classification method for brain MRI via mobilenet and feedforward network with random weights. Pattern Recognition Letters, Vol. 140, pp. 252–260. DOI: 10.1016/j.patrec.2020.10.017.
19. **López-Cabrera, J., Lorenzo-Ginori, J. (2017).** Automatic classification of traced neurons using morphological features.

Computacion y Sistemas, Vol. 21, No. 3, pp. 537–544. DOI: 10.13053/CyS-21-3-2495.

20. **McKinley, R., Wepfer, R., Grunder, L., Aschwanden, F., Fischer, T., Friedli, C., Muri, R., Rummel, C., Verma, R., Weisstanner, C., Wiestler, B., Berger, C., Eichinger, P., Muhlau, M., Reyes, M., Salmen, A., Chan, A., Wiest, R., Wagner, F. (2020).** Automatic detection of lesion load change in multiple sclerosis using convolutional neural networks with segmentation confidence. NeuroImage: Clinical, Vol. 25, pp. 102104. DOI: 10.1016/j.nicl.2019.102104.
21. **Oliva, D., Cuevas, E., Pajares, G., Zaldivar, D., Osuna, V. (2014).** A multilevel thresholding algorithm using electromagnetism optimization. Neurocomputing, Vol. 139, pp. 357–381. DOI: 10.1016/j.neucom.2014.02.020.
22. **Pasa, F., Golkov, V., Pfeiffer, F., Cremers, D., Pfeiffer, D. (2019).** Efficient deep network architectures for fast chest x-ray tuberculosis screening and visualization. Scientific Reports, Vol. 9, No. 1. DOI: 10.1038/s41598-019-42557-4.
23. **Rodríguez-Santiago, A. L., Arias-Aguilar, J. A., Takemura, H., Petrilli-Barcelo, A. E. (2021).** High-resolution reconstructions of aerial images based on deep learning. Computación y Sistemas, Vol. 25, No. 4, pp. 739–749. DOI: 10.13053/cys-25-4-4047.
24. **Ruder, S. (2016).** An overview of gradient descent optimization algorithms. DOI: 10.48550/ARXIV.1609.04747.
25. **Saurabh, S., Gupta, P. K. (2022).** Non-linear behavior of CNN model interpretation using saliency map. Proceedings of the 7th International Conference on Parallel, Distributed and Grid Computing, pp. 733–738. DOI: 10.1109/PDGC56933.2022.10053135.
26. **Saurabh, S., Gupta, P. K. (2023).** Deep learning-based modified bidirectional LSTM network for classification of ADHD disorder. Arabian Journal for Science and Engineering, Vol. 49, No. 3, pp. 3009–3026. DOI: 10.1007/s13369-023-07786-w.
27. **Shorten, C., Khoshgoftaar, T. M. (2019).** A survey on image data augmentation for deep learning. Journal of Big Data, Vol. 6, No. 1, pp. 1–48. DOI: 10.1186/s40537-019-0197-0.
28. **Simonyan, K., Vedaldi, A., Zisserman, A. (2014).** Deep inside convolutional networks: Visualising image classification models and saliency maps. Workshop at International Conference on Learning Representations.
29. **Sinha, D., El-Sharkawy, M. (2019).** Thin MobileNet: An enhanced mobilenet architecture. Proceedings of the IEEE 10th Annual Ubiquitous Computing, Electronics Mobile Communication Conference, pp. 280–285. DOI: 10.1109/UEMCON47517.2019.8993089.
30. **Tousignant, A., Lemaître, P., Precup, D., Arnold, D. L., Arbel, T. (2019).** Prediction of disease progression in multiple sclerosis patients using deep learning analysis of MRI data. Proceedings of the 2nd International Conference on Medical Imaging with Deep Learning, Vol. 102, pp. 483–492.
31. **Varela, E., Moya-Sanchez, E. U., Aguilar-Meléndez, A., Castillo Reyes, O., Vázquez-Santacruz, E., Salazar-Colores, S., Cortés, U. (2019).** Detection, counting, and classification of visual ganglia columns of drosophila pupae. Computación y Sistemas, Vol. 23, No. 2, pp. 391–397. DOI: 10.13053/CyS-23-2-3200.
32. **Zhang, Y. D., Pan, C., Sun, J., Tang, C. (2018).** Multiple sclerosis identification by convolutional neural network with dropout and parametric ReLU. Journal of Computational Science, Vol. 28, pp. 1–10. DOI: 10.1016/j.jocs.2018.07.003.

Article received on 25/03/2022; accepted on 21/07/2024.
**Corresponding author is Sudhanshu Saurabh.*